



UNIVERSITÀ
DEGLI STUDI
FIRENZE

FLORE

Repository istituzionale dell'Università degli Studi di Firenze

Small-angle neutron scattering of Ca(AOT)_2-D_2O-decane microemulsions

Questa è la Versione finale referata (Post print/Accepted manuscript) della seguente pubblicazione:

Original Citation:

Small-angle neutron scattering of Ca(AOT)_2-D_2O-decane microemulsions / G.Capuzzi; F.Pini; C.M.C.Gambi; M.Monduzzi; P.Baglioni. - In: LANGMUIR. - ISSN 0743-7463. - STAMPA. - 13:(1997), pp. 6927-6930.

Availability:

The webpage <https://hdl.handle.net/2158/347221> of the repository was last updated on

Terms of use:

Open Access

La pubblicazione è resa disponibile sotto le norme e i termini della licenza di deposito, secondo quanto stabilito dalla Policy per l'accesso aperto dell'Università degli Studi di Firenze (<https://www.sba.unifi.it/upload/policy-oa-2016-1.pdf>)

Publisher copyright claim:

La data sopra indicata si riferisce all'ultimo aggiornamento della scheda del Repository FloRe - The above-mentioned date refers to the last update of the record in the Institutional Repository FloRe

(Article begins on next page)

Small-Angle Neutron Scattering of Ca(AOT)₂/D₂O/Decane Microemulsions

G. Capuzzi, F. Pini, C. M. C. Gambi, M. Monduzzi, and P. Baglioni

Departments of Chemistry and Physics, University of Florence,
50121 Florence, Italy, and Department of Chemical Sciences,
University of Cagliari, 09100 Cagliari, Italy

J. Teixeira

Laboratoire Léon Brillouin, CEA-CNRS, CEN-Saclay,
91191 Gif-sur-Yvette, France

Langmuir[®]
The ACS Journal of Surfaces and Colloids

Reprinted from
Volume 13, Number 26, Pages 6927–6930

Small-Angle Neutron Scattering of $\text{Ca}(\text{AOT})_2/\text{D}_2\text{O}/\text{Decane}$ Microemulsions

G. Capuzzi,[†] F. Pini,[†] C. M. C. Gambi,[‡] M. Monduzzi,[§] and P. Baglioni^{*,†}

Departments of Chemistry and Physics, University of Florence, 50121 Florence, Italy, and
Department of Chemical Sciences, University of Cagliari, 09100 Cagliari, Italy

J. Teixeira

Laboratoire Léon Brillouin, CEA-CNRS, CEN-Saclay, 91191 Gif-sur-Yvette, France

Received May 28, 1997. In Final Form: October 2, 1997[®]

Small-angle neutron scattering (SANS) studies were performed in order to investigate the structural properties of the monophasic domain of the $\text{Ca}(\text{AOT})_2/\text{water}/\text{decane}$ phase diagram, which shows a consistent reduction of the microemulsion region as compared to the parent sodium system. Microemulsions of $\text{Ca}(\text{AOT})_2/\text{D}_2\text{O}/\text{decane}$ and $\text{Ca}(\text{AOT})_2/\text{H}_2\text{O}/\text{decane}-d_{22}$ have been studied at 25 °C, for an oil dilution line at constant $[\text{water}]/[\text{Ca}(\text{AOT})_2] = 25.1$, as a function of decane concentration and of surfactant volume fraction, ϕ_s , in the range $0.0186 \leq \phi_s < 0.0937$ for the D_2O system, or $0.0249 \leq \phi_s \leq 0.0886$ for the corresponding decane- d_{22} system. SANS spectra were analyzed according to a self-consistent method proposed by Sheu¹ and support, in analogy to the sodium AOT microemulsion system, the presence of polydisperse droplets in the diluted region studied, while the system shows a percolative behavior for higher concentrations. These droplets have a 21.3 Å average radius with polydispersity around 22%. The mean area per polar head group and the principal geometrical parameters are also reported.

Introduction

Water in oil microemulsions are thermodynamically stable mixtures of oil, water, and surfactant. They are formed by water and oil domains separated by a surfactant monolayer and are isotropic and homogeneous on a macroscopic scale but heterogeneous on a molecular scale. These complex fluids have a wide range of applications, as cell analogues in biotechnology, as lubricants, in the foods and cosmetic industries, etc.

The sodium salt of the dichained anionic surfactant bis-(2-ethylhexyl)sulfosuccinate (Aerosol OT or simply NaAOT) is well-known to form water-in-oil microemulsions in a wide range of temperatures and compositions. Many studies on the structure and dynamic of AOT microemulsions have been extensively carried out as a function of several parameters such as surfactant concentration, temperature, type of oil,^{2–4} etc. The results provided significant advances in understanding phase transitions, critical phenomena, percolation theory, the role of the interparticle interactions on the structure and dynamics of colloidal and molecular fluids, and protein, enzyme, and whole cell solubilization in the confined water pool of microemulsions.⁵

It is well-known that electrostatic forces strongly affect the size and shape of the aggregates. Counterion effects on microemulsions formed by divalent metal ions aerosol–

AOT surfactants have been studied and compared to sodium AOT. The main difference between the binary system calcium–AOT/water and the sodium–AOT/water system is a significant reduction of the extension of the lamellar (L_a) region.^{6,7} At 25 °C the monophasic L_a phase occurs at about 13% and 65% (by weight) for NaAOT and $\text{Ca}(\text{AOT})_2$ respectively. These L_a phases are stable up to about 100 °C for $\text{Ca}(\text{AOT})_2$ and up to 160 °C for NaAOT. Minor differences in the formation and range of existence of the bicontinuous cubic V_2 and reverse hexagonal H_2 phases are observed. These findings agree with theoretical Poisson–Boltzmann and Monte Carlo calculations which predict substantially smaller interlamellar repulsion with divalent than with monovalent counterions.⁸ This, in turn, decreases capability of the $\text{Ca}(\text{AOT})_2$ L_a -phase to swell and to incorporate as much water as in the case of NaAOT.⁸

Some authors⁹ studied the $\text{M}^{2+}(\text{AOT})_2$ system for a wide number of ions, as Co^{2+} , Ni^{2+} , Cu^{2+} , Zn^{2+} , Cd^{2+} , Mg^{2+} , and Ca^{2+} , showing that counterion identity strongly influences the shape of the micellar aggregates. The form-factor, determined by small-angle neutron scattering (SANS) on the $\text{M}(\text{AOT})_2$ systems with water to surfactant head group mole ratio $w_0 = 5$, provides evidence of the structural changes from the simple hard-sphere micelle for Na^+ and Ca^{2+} , to rod-shaped cylindrical micelle for Co^{2+} , Ni^{2+} , Cu^{2+} , and Zn^{2+} , through intermediate shapes for Mg^{2+} and Cd^{2+} ions.

This work investigates the effects induced on the microemulsion structure by exchanging Na^+ with Ca^{2+} . We compare the $\text{Ca}(\text{AOT})_2/\text{water}/\text{decane}$ system with the well-known NaAOT/water/decane system,^{10–13} with particular regard to the surfactant diluted region.

* Corresponding author: Department of Chemistry, University of Florence, Via Gino Capponi 9, 50121 Florence, Italy; e-mail, colloid@sirio.cineca.it; http://mac.chim.unifi.it; fax, +39.55.240865; voice, +39.55.2757567.

[†] Department of Chemistry, University of Florence.

[‡] Department of Physics, University of Florence.

[§] Department of Chemical Sciences, University of Cagliari.

[®] Abstract published in *Advance ACS Abstracts*, November 15, 1997.

(1) Sheu, E. Y. *Phys. Rev. A* **1992**, *45* (4), 2428–38.

(2) Kotlarchyk, M.; Chen, S.-H.; Huang, J. S. *Phys. Rev. A* **1984**, *29*, 2054.

(3) Ekwall, P.; Mandell, L.; Fontell, K. *J. Colloid Interface Sci.* **1970**, *33* (2), 215.

(4) Eastoe, J.; Robinson, B. H.; Steyler, D. C.; Young, W. K. *J. Chem. Soc., Faraday Trans.* **1990**, *86*, 2883.

(5) Migliardo, P. *J. Mol. Struct.* **1993**, *296*, 229.

(6) Khan, A.; Fontell, K.; Lindman, B. *J. Colloid Interface Sci.* **1984**, *101* (1), 193.

(7) Khan, A.; Jönsson, B.; Wennerström, H. *J. Phys. Chem.* **1985**, *89*, 5180.

(8) Franses, E. I.; Hart, T. J. *J. Colloid Interface Sci.* **1983**, *94*, 1–13.

(9) Eastoe, J.; Towey, T. F.; Robinson, B. H.; Williams, J.; Heenan, R. K. *J. Phys. Chem.* **1993**, *97*, 1459.

(10) Kotlarchyk, M.; Chen, S. H.; Huang, J. S.; Kim, M. W. *Phys. Rev. Lett.* **1984**, *53* (9), 941.

(11) Kotlarchyk, M.; Chen, S. H.; Huang, J. S.; Kim, M. W. *Phys. Rev. A* **1984**, *29* (4), 2054.

(12) Chen, S. H. *Annu. Rev. Phys. Chem.* **1986**, *37*, 351–99.

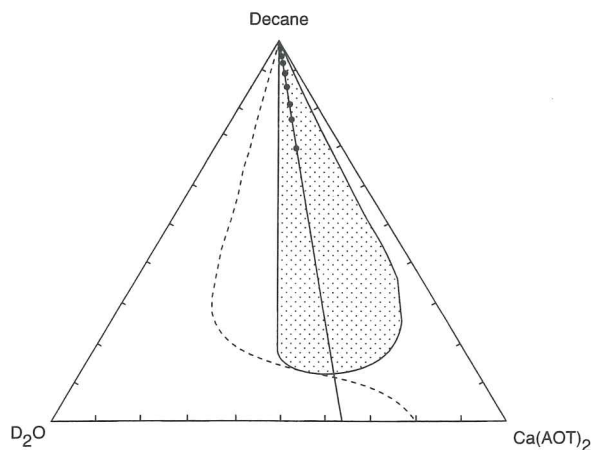


Figure 1. Phase Diagram of the $\text{Ca(AOT)}_2/\text{D}_2\text{O}/\text{decane}$ microemulsion system. The $\text{NaAOT}/\text{D}_2\text{O}/\text{decane}$ microemulsion region (dashed line) is reported for comparison. The oil dilution line with water-to-surfactant ratio $w/s = 25$ or water-to-polar head group ratio $[\text{water}]/[\text{AOT}^-] = 12.5$ is also reported. The symbols represent the measured samples.

In particular, the analysis of SANS measurements for two different sets of samples ($\text{D}_2\text{O}/\text{decane}$ and $\text{H}_2\text{O}/\text{decane-}d_{22}$) along the same oil dilution line is reported. These measurements are analyzed according to the self-consistent method proposed by Sheu,¹ using a Schultz distribution to take into account the particle polydispersity. Guinier's law, modified to include the particle size distribution, and Porod's law were also used to obtain the geometrical parameters as surface area of the surfactant polar head groups at the interface, surfactant tail length, and oil penetration into the surfactant corona of the microemulsion droplet.

Experimental Section

The calcium salt of AOT was prepared by aqueous metathesis of a saturated solution of $\text{Ca(NO}_3)_2$ (Aldrich AR) with an ethanolic solution of NaAOT (Sigma). The Ca(AOT)_2 precipitate was separated from the aqueous phase by settling and washed repeatedly with Millipore filtered bidistilled water (conductivity $< 10^{-6} \Omega^{-1} \text{cm}^{-1}$ at 25°C) until complete disappearance of NO_3^- (determined by the brown ring test) and Na^+ (atomic adsorption spectroscopy) ions. The remaining water was eliminated by freeze-drying. The single-phase region diagram was obtained studying the phase behavior at 25°C of samples with oil to surfactant weight ratio constant by increasing the content of deuterated water. The Ca(AOT)_2 microemulsion region appears narrower than that of NaAOT, underlining consistent differences produced from the exchange of Na^+ with Ca^{2+} counterion (see Figure 1).

Sample preparation was carried out using deuterium oxide (deuterium content $> 99.99\%$, Carlo Erba) and *n*-decane (purity $> 99\%$ olefin free, Fluka AG), Millipore filtered bidistilled H_2O and deuterated decane (D atom at 99% , Euriso-top).

SANS measurements have been performed on the PAXE spectrometer of the Laboratoire Léon Brillouin at Saclay (France) using a wavelength of 5 \AA with a wavelength spread, $\Delta\lambda/\lambda$, less than 10% . The Q range investigated, for all samples, was $0.01 < Q < 0.36 \text{ \AA}^{-1}$, with a sample to detector distance of 2.3 m . Samples were contained in 1 mm flat quartz cells at the controlled temperature of $25 \pm 0.1^\circ\text{C}$. The intensity, corrected for the empty cell contribution, was normalized to absolute scale by a known cross section standard.

Results and Discussion

This paper reports preliminary results on the structure of the $\text{Ca(AOT)}_2/\text{water}/\text{decane}$ microemulsion system. All measurements have been performed at 25°C for samples

along the oil dilution line with $[\text{water}]/[\text{Ca(AOT)}_2] = 25.1$ and surfactant volume fraction $0.0258 \leq \phi_s < 0.0937$.

In order to define the thickness of the AOT hydrocarbon chain, and therefore the oil penetration into the AOT chain, we have also performed some measurements on the $\text{Ca(AOT)}_2/\text{H}_2\text{O}/\text{decane-}d_{22}$ system with surfactant volume fraction $0.0249 \leq \phi_s \leq 0.0886$.

SANS analysis was performed according to Sheu¹ to minimize the occurrence of multiple convergence and consisted of four steps: (1) assumption of a functional form factor for particle distribution (in our case Schultz distribution describes very well the particle-size distribution); (2) calculation of the scattering intensity distribution function and (3) fitting of the experimental data to extract polydispersity and structural parameters; (4) calculation of the average particle-solvent scattering contrast, according to the presumed particle distribution function. This procedure was repeated for different particle concentrations and different contrast (D_2O or $\text{decane-}d_{22}$).

For a number N_p of monodisperse particles, the normalized SANS intensity, $I(Q) (\text{cm}^{-1})$, may be written as

$$I(Q) = N_p \langle P(Q) \rangle \langle S(Q) \rangle \quad (1)$$

$P(Q)$ is the intraparticle structure factor describing the normalized angular distribution of the scattering owing to the size and shape of the particle. $S(Q)$ is the structure factor which arises from interference effects due to spatial correlations between particles.

For diluted samples, one can consider that the system becomes ideal and $S(Q) \approx 1$, so that

$$I(Q) \approx N_p \langle P(Q) \rangle \quad (2)$$

For the case of an isotropic system containing homogeneous but polydisperse spherical particles, the form factor can be written as¹⁴

$$P(Q) = \int_0^\infty |F(Q,R)|^2 f(R) dR \quad (3)$$

where

$$F(Q,R) = [3j_1(QR)/QR] \quad (4)$$

$F(Q,R)$, the particle form factor for a sphere of radius R , depends on the first-order spherical Bessel function $j_1(QR)$ and $f(R)$ is the Schultz distribution function of a sphere having a radius between R and $R + dR$.

The probability function, $f(R)$, is the two-parameter-function Schultz distribution

$$f(R) = \left[\frac{R^Z}{\Gamma(Z+1)} \right] \left[\frac{(Z+1)}{R} \right]^{Z+1} \exp \left[-\frac{(Z+1)R}{\bar{R}} \right] \quad (5)$$

where \bar{R} is the mean of the distribution and Z is a width parameter which is $Z > -1$, and $\Gamma(Z+1)$ is the gamma function. The function tends to a Gaussian form at large values of Z and the distribution approaches a delta function at $R = \bar{R}$ as Z approaches infinity. The root mean square deviation from the mean is given by

$$\sigma_R = (\overline{R^2} - \bar{R}^2)^{1/2} = \bar{R}/(Z+1)^{1/2} \quad (6)$$

which is related to the polydispersity of the system.

Therefore, considering a polydisperse particles system, the form factor $P(Q)$ spherically averaged can be developed in the Taylor series

(13) Eastoe, J.; Young, W. K.; Robinson, B. H.; Steytler, D. C. *J. Chem. Soc., Faraday Trans.* **1990**, *86* (16), 2883.

(14) Kotlarchyk, M.; Chen, S. H. *J. Chem. Phys.* **1983**, *79* (5), 2461.

$$P(Q) = 1 - (Q\bar{R})^2/5 + \dots \cong \exp(-\epsilon(Q\bar{R})^2/5) \quad (7)$$

where the parameter $\epsilon = [(Z + 8)(Z + 7)]/(Z + 1)^2$ is introduced to take into account the polydispersity.

Equation 7 represent the Guinier equation¹⁵ corrected for polydisperse systems. The parameter ϵ assumes values usually larger than 1, therefore, neglecting polydispersity ($\epsilon = 1$) can lead to an overestimate of the mean particle size.

Figure 2 shows the excellent agreement between the experimental and calculated spectra assuming a Schultz distribution for polydisperse droplets. A similar agreement was found for all the samples investigated. A good agreement between the experimental and calculated spectra was also found using a monodisperse cylindrical model as form factor (see Figure 2). The data extracted from the fitting do not show dependence from the concentration and the average parameters characterizing the microemulsion system are reported in Table 1. As stated above, both the spherical Schultz model and monodisperse cylindrical model can fit the data. However, the convergence values between calculated and experimental data, χ^2 , for the spherical model are lower than those obtained by assuming a monodisperse cylindrical model for the particle form factor. In order to remove ambiguity on the particle form factor, we calculated the structural parameter A_0 , which is independent from concentration when the size distribution is appropriate.

$$A_0 = (A/C_w)(\langle V_p \rangle / \langle V_p^2 \rangle) = (\Delta\rho)^2/k \quad (8)$$

The A_0 values, obtained for different surfactant concentrations, are independent of the concentration, and the standard deviation from the average value is around 4% for polydisperse sphere and around 14% for monodisperse cylinder (see Figure 3), supporting that the $\text{Ca}(\text{AOT})_2$ system is formed of polydisperse spherical particles.

In conclusion the $\text{Ca}(\text{AOT})_2/\text{D}_2\text{O}/\text{decane}$ system is formed of polydisperse spheres of 21.3 Å average radius and 22% polydispersity. The simple Guinier's analysis, not corrected for polydispersity, would give 26 Å, and 20 Å considering polydispersity.

Chen¹² derived a semiempirical relationship to calculate the average water core radius of polydisperse sphere, \bar{R} , for the $\text{Na}(\text{AOT})/\text{D}_2\text{O}/\text{decane}$. \bar{R} can be calculated according to the following relationship

$$(1 + 2p^2)\bar{R} = \frac{3V_w}{a_H}w_0 + \frac{3V_H}{a_H} \quad (9)$$

where $w_0 = [\text{water}]/[\text{surfactant polar head group}]$, V_w is the molar volume of deuterated water, V_H and a_H are the volume and the area of the polar head group of AOT molecule, and $p = (Z + 1)^{-1/2}$ is the polydispersity.

Using the geometrical parameters of $\text{Ca}(\text{AOT})_2$ and the w_0 value corrected for the critical micelle concentration (cmc) of $\text{Ca}(\text{AOT})_2$ (0.024 mol/dm³) we obtain a radius $\bar{R} = 21.1$ Å, in good agreement with the values obtained using the Schultz distribution and Guinier's equation.

The analysis of Table 1 shows that the average radius obtained for $\text{Ca}(\text{AOT})_2/\text{H}_2\text{O}/\text{decane-}d_{22}$ microemulsion droplets is 26.5 Å with a 20% polydispersity. This value differs by about 5 Å from the corresponding radius of $\text{Ca}(\text{AOT})_2/\text{D}_2\text{O}/\text{decane}$. It is worthwhile to recall that the different contrast, due to the exchange of D_2O with H_2O and decane with decane- d_{22} , allows detection of different regions of the microemulsion droplets, i.e., water droplets

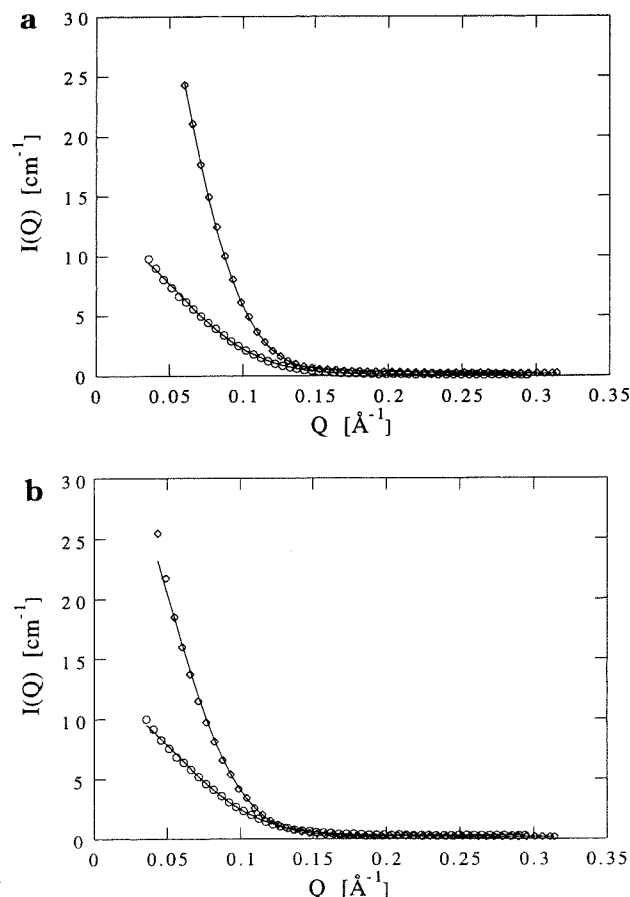


Figure 2. Experimental (symbols) and calculated (lines) SANS spectra of $\text{Ca}(\text{AOT})_2/\text{water}/\text{decane}$ microemulsions: (●) $\text{Ca}(\text{AOT})_2/\text{D}_2\text{O}/\text{decane}$; (◆) $\text{Ca}(\text{AOT})_2/\text{H}_2\text{O}/\text{decane-}d_{22}$. Data fitting assuming (a) a spherical form factor with a Schultz polydispersity and (b) a monodisperse cylindrical model.

Table 1. Parameters Obtained from the Analysis of SANS Data Using a Spherical Schultz Distribution and a Monodisperse Cylindrical Model for the Form Factor of $\text{Ca}(\text{AOT})_2/\text{Water}/\text{Decane}$ Microemulsion Systems: (a) $\text{Ca}(\text{AOT})_2/\text{D}_2\text{O}/\text{Decane}$ and (b) $\text{Ca}(\text{AOT})_2/\text{H}_2\text{O}/\text{Decane-}d_{22}$

	(a)	(b)
Spherical Form Factor		
volume (Å ³)	40.7×10^3	85×10^3
background (cm ⁻¹)	1.055	0.11
Z	20	24
radius (Å)	21.3	26.5
polydispersity	22%	20%
ϵ	1.714	1.587
R_H (Guinier) (Å)	19.8	26.6
Monodisperse Cylinders		
volume (Å ³)	95×10^3	160×10^3
background (cm ⁻¹)	1.076	0.136
radius (Å)	27.7	33.1
h/diameter	1.26	1.15
h (Å)	69.8	76.13

plus AOT polar head groups and water droplets plus AOT corona, respectively. Therefore, the alkyl chain length of the $\text{Ca}(\text{AOT})_2$ is about 5 Å, shorter than the extended AOT chain length, which is about 8 Å. This suggests that about 3 Å of the AOT chain length is penetrated by decane, while the corresponding $\text{Na}(\text{AOT})$ system exhibits a lower oil penetration (1–2 Å).¹⁶ This can be explained by considering that Ca^{2+} counterion coordinates two AOT⁻ ions, imposing a larger interfacial curvature as compared

(15) Guinier, A.; Fournier, G. *Small-angle Scattering of x-ray*; J. Wiley: New York, 1955.

(16) Chen, S.-H.; Lin, T.-L.; Huang, J. S. In *Physics of Complex and Supramolecular Fluids*; Safran and Clark, Eds.; Wiley Interscience Publication: J. Wiley & Sons: New York, 1987.

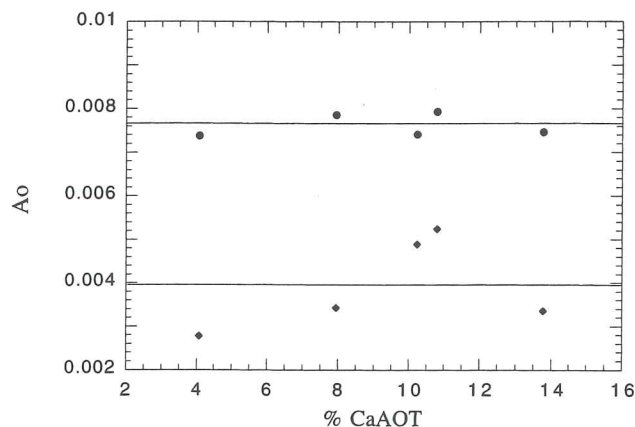


Figure 3. A_0 values as a function of $\text{Ca}(\text{AOT})_2$ concentration (% w/w) for the spherical model with Schultz distribution (●) and cylindrical model (◆). The A_0 values fluctuate at about 4% and 14% around the mean value (continuous line) for spherical form factor with a Schultz polydispersity and monodisperse cylindrical form factor, respectively.

to sodium counterion. The stiffness of the AOT corona decreases, due to the larger oil penetration into the surfactant layer, leading to higher $\text{Ca}(\text{AOT})_2$ solubility in decane and probably to different interdroplet interactions.

At large wave vector, typically $Q > 0.20 \text{ \AA}^{-1}$, SANS is sensitive to the scattering from the interface and the asymptotic intensity may be analyzed using the model-independent Porod's equation¹⁷

$$I(Q) = 2\pi(\Delta\rho)^2 c_S \Sigma Q^4 + I(Q)_{\text{bkg}} \quad (10)$$

where c_S is the surfactant concentration per unit volume of solution and $c_S \Sigma = S/V$ is the total interfacial area per unit volume of the surfactant. This law can be written in the form:¹⁸

$$I(Q)Q^4 = 2\pi(\Delta\rho)^2 c_S \Sigma + BQ^{-4} \quad (11)$$

where the term $B = I(Q)_{\text{bkg}}$ accounts for the incoherent contribution of the hydrogen atoms of the sample as well as any incoherent part. The fitting of the experimental data to the latter relationship allows the calculation of $A = 2\pi(\Delta\rho)^2 c_S \Sigma$ and B . Once the scattering contrast $\Delta\rho$ and the c_S values are known, Σ can be obtained from A . Σ is related to a_H , the mean area per AOT^- group at the interface, via the number density of AOT^- , N_S , corrected for the cmc value

$$a_H = \Sigma/N_S = (S/V)/N_S \quad (12)$$

The analysis of $\text{Ca}(\text{AOT})_2/\text{D}_2\text{O}/\text{decane}$ microemulsion SANS spectra in terms of eqs 11 and 12 gives an area per polar head group of $116 \text{ \AA}^2/\text{molecule}$ and an aggregation number of about 50.

This result can be compared with the area obtained from the structural analysis above reported. For a polydisperse system, the area per polar head group can be calculated considering that the average surface area is given by

$$\int_0^\infty S(R)f(R) dR \quad (13)$$

where $f(x)$ is the Schultz distribution (see eq 5) that accounts for the particle polydispersity. Substitution in the integral gives

$$\langle S \rangle = \left[\frac{4\pi}{\Gamma(Z+1)} \left(\frac{\bar{R}}{Z+1} \right)^2 \Gamma(Z+3) \right] \quad (14)$$

and

$$a_H = \frac{\langle S \rangle}{N} \left[4\pi \frac{(Z+2)}{(Z+1)} \bar{R}^2 \right] \quad (15)$$

The aggregation number, N , can be obtained from the total volume fraction of the dispersed D_2O and is found to be about 54. Thus, the area per polar head group calculated from the structural analysis is $a_H = 111 \text{ \AA}^2/\text{molecule}$, in excellent agreement with that obtained from Porod analysis ($116 \text{ \AA}^2/\text{molecule}$).

Conclusions

The substitution of Na^+ with Ca^{2+} produces a consistent reduction of the microemulsion domain of the phase diagram of the ternary $\text{Ca}(\text{AOT})_2/\text{D}_2\text{O}/\text{decane}$ system (see Figure 1). The analysis of the small angle scattering results shows that, in analogy to the sodium microemulsion system, the ternary $\text{Ca}(\text{AOT})_2/\text{D}_2\text{O}/\text{decane}$ system is formed of polydisperse spherical water droplets with an average radius of 21.3 \AA and a polydispersity of 22%.

$\text{Ca}(\text{AOT})_2$ microemulsions are formed of smaller droplets, have a lower polydispersity, and have a larger oil penetration into the AOT alkyl chain than the corresponding $\text{Na}(\text{AOT})$ system. This analysis was successfully performed by using Sheu's¹ method, which is one of the methods for polydisperse analysis with a reasonably good sensitivity in differentiating various models.

The overall $\text{Ca}(\text{AOT})_2$ microemulsion structural feature is very similar to that of sodium. Therefore, the variation of the AOT phase diagram due to the exchange of Na^+ with Ca^{2+} and, in particular, the strong reduction of the isotropic region in the phase diagram should be related to different interdroplet interactions.

Acknowledgment. The authors thank the "Consorzio per lo Sviluppo dei Sistemi a Grande Interfase" (C.S.G.I.), MURST, and CNR for financial support. G.C. thanks the C.S.G.I. for a fellowship. Acknowledgment is also due to the European Community for support via the "HCM-Access to large scale facilities" program (ERB CHGECT 920001).

LA970561C

(17) Porod, G. *Kolloid-Z.* **1951**, *124*, 83.

(18) Auvray, L. *Micelles, Membrane, Microemulsions, and Monolayers*; Gelbart, W. M., Roux, D., Ben-Shaul, A., Eds.; Springer-Verlag: New York, 1994.